ADVANCED MATERIALS
www.advmat.de

Harmonic-Resonator-Based Triboelectric Nanogenerator as a Sustainable Power Source and a Self-Powered Active Vibration Sensor

*Jun Chen, Guang Zhu, Weiqing Yang, Qingshen Jing, Peng Bai, Ya Yang, Te-Chien Hou, and Zhong Lin Wang**

Energy harvesting of ambient wasted energy addresses limitations of traditional power supplies by providing a supplementary electric power source. Vibration, as a type of common mechanical motion, is ubiquitous in daily life, from operating household appliances, such as washing machines and refrigerators, to bouncing automobile tires on a gravel road. In recent years, it has become an attractive target for energy harvesting as a potentially alternative power source for battery-operated electronics. Until recently, the mechanisms of vibrational energy harvesting have been limited to transductions based on piezoelectric effect,[1–5] electromagnetic effect,[6] electrostatic effect,[7] and magnetostrictive effect.[8] Widespread usage of these techniques is likely to be shadowed by possible limitations, such as structure complexity,[9] fabrication of high-quality materials,[10] and reliance on external power source.[9] Furthermore, all of the mechanisms require energy-harvesting devices to operate at or within a very narrow range around resonance frequency. However, most ambient vibrations have a wide distribution of frequency spectrum, which may even drift over time, making the conventional mechanisms unsuitable in most circumstance. Generally, an effective vibrational energy harvester needs to meet at least two criteria.[11] First, it can be applicable to a broad range of vibration frequency instead of a single resonance frequency. Second, it can effectively respond to vibrations at low frequency (below a few hundred Hz), as most ambient vibrations lie in this range (the natural oscillation frequencies range from 1–10 Hz for human motion and 10–100 Hz for machine-induced vibrations).[12]

Recently, triboelectric nanogenerators (TENGs),[13–22] which are creative inventions for harvesting ambient mechanical energy on the basis of the triboelectric effect,[23–25] have proved to be a cost-effective, simple, and robust technique for self-powered devices and systems. Owing to coupling between the triboelectric effect and electrostatic induction, the periodic contact and separation between two materials with opposite triboelectric polarities alternatingly drives the induced electrons between electrodes.

Here, we introduce a new principle in harvesting vibration energy by fabricating a harmonic-resonator-based TENG. It is the first TENG that can harness random and tiny ambient vibration, which is the most common and usually the sole available mechanical source for self-powered electronics, especially in wireless sensor applications. The rationally designed TENG, operating at resonance frequency, produces a uniform quasi-sinusoidal signal output at an open-circuit voltage up to 287.4 V and a short-circuit current amplitude of 76.8 μA, corresponding to a peak power density of 726.1 mW m^{-2}. Compared to state-of-the-art nonlinear and topology-variation-based vibration energy harvesters,[26–28] it has a considerably wider working bandwidth of 13.4 Hz in low frequency range. It has proved to be effective in harvesting energy from common ambient vibrations including car engine and household furniture. With vibration amplitude less than 3 mm, it can still deliver stable electric output after operating for more than 1 million cycles (Figure S2, Supporting Information). In addition, the TENG can also act as a self-powered active sensor for detecting ambient vibration, such as roadside vibration triggered by normal human walking. The concept and design presented in this work can be further applied in various other circumstances for either energy-harvesting or sensing purposes: for example, highways, bridges, and tunnels. Therefore, it is a milestone in the development towards TENG-based self-powered electronics.

The harmonic-resonator-based TENG has a multilayer structure with acrylic as supporting substrates, as schematically shown in **Figure 1**a. Acrylic was selected as the structural material owing to its decent strength, light weight, good machinability, and low cost. A photograph of an as-fabricated TENG is shown in Figure 1b. On the upper substrate, aluminum thin film with nanoporous surface has dual roles as an electrode and a contact surface. A scanning electron microscopy (SEM) image of nanopores on the aluminum is presented in Figure 1c. The average diameter of aluminum nanopores are 57 ± 5 nm and a pore depth of 0.8 ± 0.2 μm with a distribution density of 212 μm^{-2}. A layer of polytetrafluoroethylene (PTFE) film was adhered to the lower substrate with deposited copper as another electrode. PTFE nanowires arrays were created on the exposed PTFE surface by a top-down method through reactive ion etching. SEM image of the PTFE nanowires is displayed in the Figure 1d. The average diameter of PTFE nanowires is 54 ± 3 nm with an average length of 1.5 ± 0.5 μm. The

J. Chen, G. Zhu, W. Yang, Q. Jing,
P. Bai, Y. Yang, T.-C. Hou, Prof. Z. L. Wang
School of Materials Science and Engineering
Georgia Institute of Technology
Atlanta, GA 30332, USA
E-mail: zlwang@gatech.edu
Prof. Z. L. Wang
Beijing Institute of Nanoenergy and Nanosystems
Chinese Academy of Sciences, Beijing, China

DOI: 10.1002/adma.201302397

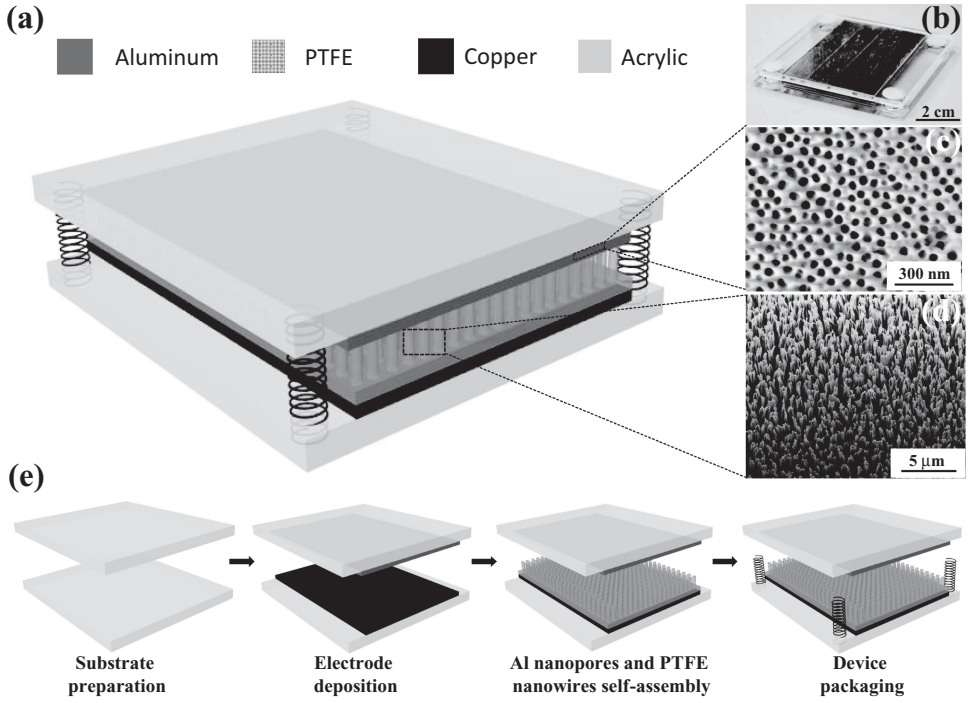

Figure 1. Harmonic-resonator-based triboelectric nanogenerator. a) A sketch and b) a photograph of a typical harmonic-resonator-based TENG. c) An SEM image of nanopores on aluminum electrode. d) An SEM image of PTFE nanowires. e) Process flow for fabricating the harmonic-resonator-based TENG.

fabrication process for the TENG is sketched in Figure 1e and discussed in details in the Experimental Section.

To operate, the bottom substrate of the TENG is attached to an external vibrational source. A cycle of electricity generation process is illustrated in **Figure 2**. At original position, the PTFE layer is in contact with the aluminum thin film. Because PTFE is much more triboelectrically negative than aluminum, electrons are injected from aluminum into PTFE, generating positive triboelectric charges on the aluminum side and negative charges on the PTFE side (Figure 2a).[13–15,29,30] Once an external vibration acts on the TENG, it accelerates and moves upwards. After the vibration source reaches the crest point, the lower substrate attached to the vibration source ceases to rise and starts dropping downwards. However, the upper substrate keeps moving up owing to its inertia. Thus, the two substrates move apart, leading to a separation between the PTFE and the aluminum. As a result, the positive triboelectric charges and the negative ones no longer coincide on the same plane and generate an inner dipole moment between the two contact surfaces. Such a dipole moment drives free electrons from the copper electrode to the aluminum electrode to balance out the electric field, producing positively induced charge on the copper electrode (Figure 2b). The flow of electrons lasts until the upper substrate reaches the highest point, where the corresponding separation is maximized (Figure 2c). Subsequently, the upper substrate is pulled downwards by the restoring force from the four stretched springs at corners. In reponse to the reduced seperation and thus to the weakened dipole moment, free electrons flow back to the copper electrode until the two contact surfaces come into collision, making a complete cycle of electricity generation process (Figure 2d). The upper electrode is then bounced upwards again after obtaining a momentum from the collision, starting another cycle. Therefore, the TENG acts as an electron pump that drives electrons back and forth between electrodes, producing alternating current in the external circuit.

To investigate the performance of the TENG in harvesting vibration energy, an electrodynamic shaker (from Labworks Inc.) that provides a sinusoidal wave was used as a vibration source with tunable frequency and amplitude. The lower substrate of the TENG was anchored on the shaker, leaving the the upper part free-standing. At a fixed vibration amplitude, the reliance of electric output on the input vibration frequency is presented in **Figure 3**a and Figure 3b. The electric output can be measured with broad input frequencies varying from 2 to 200 Hz. Compared to state-of-the-art vibration energy harvesters that are based on nonlinear and topology variation,[26–28] it has a considerably wider working bandwidth of 13.4 Hz (see Figure S3, Supporting Information).

Experimentally, both the open-circuit voltage (V_{oc}) and the short-circuit current (I_{sc}) are maximized at the vibration frequency of 14.5 Hz with maximum values of 287.4 V and 76.8 μA, respectively, indicating that 14.5 Hz is the resonance frequency of the TENG. Theoretically, for a single degree-of-freedom vibration system, the natural frequency is given by (see Supporting Information for detailed derivation):[31]

$$f_0 = \frac{1}{2\pi}\sqrt{\frac{4k}{m_0}} \quad (1)$$

Adv. Mater. **2013**,
DOI: 10.1002/adma.201302397

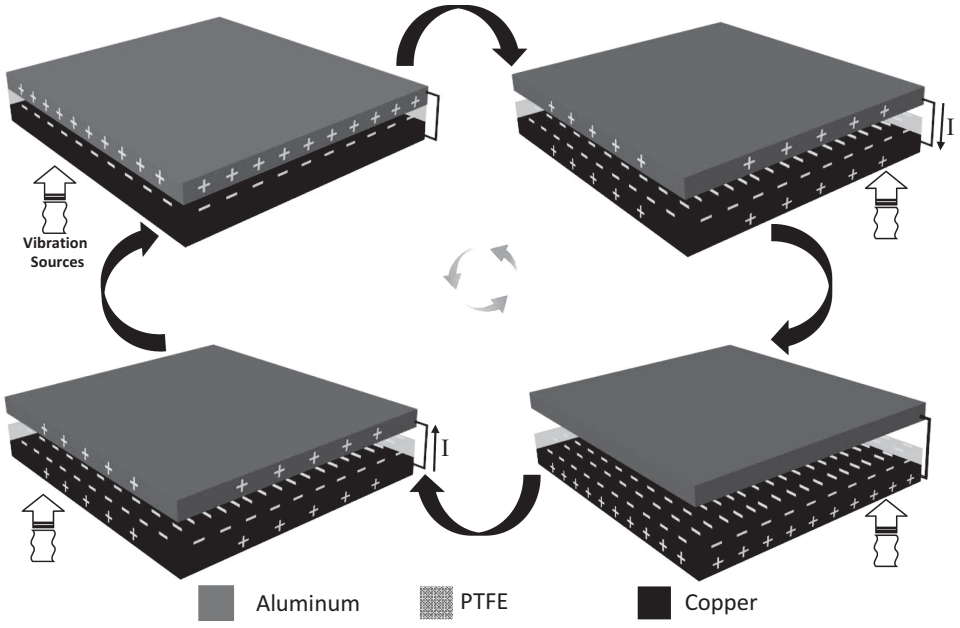

Figure 2. A cycle of electricity generation process for illustrating the working mechanism of the harmonic-resonator-based TENG. a) Critical position with the springs' elastic force exactly compensating the gravitational force of the top plate and the two plates just in contact with each other, generating positive triboelectric charges on the aluminum side and negative charges on the PTFE side. b) External vibration separates the PTFE and aluminum. Electric potential difference drives the electrons from the back electrode to the contact electrode, screening the triboelectric charges and leaving behind the inductive charges. c) With continuously increasing the separation, all of the positive triboelectric charges are gradually and almost entirely screened. d) Electrons are driven back to the back electrode owing to the applied external vibration, screening the inductive charges. Notes: aluminum nanopores, PTFE nanowires and springs are not shown in the sketch for the simplification of illustration.

where f_0 is the natural frequency, m_0 is the mass of the upper substrate plus the aluminum film, and k is the stiffness coefficient of each spring. For the TENG, m_0 is 56.8 g, and the spring stiffness coefficient is 112 N m^{-1}. Inputting the values into Equation (1), we can obtain the natural frequency f_0 of 14.1Hz, which is consistent with the experimental result.

At the resonance frequency, the V_{oc} is elaborated in Figure 3c. It has a uniform quasi-sinusoidal signal owing to the fact that the upper substrate of the TENG vibrates in a harmonic manner. Theoretically, the harmonic-resonator-based TENG can be regarded as a damped system subjected to a harmonically varying force. Therefore, the maximum V_{oc} at the resonance frequency can be expressed as (see Supporting Information for detailed derivation of the analytical model):

$$V_{oc-rf} = \frac{\sigma}{\varepsilon_0} \cdot \frac{m_0 a}{2k\zeta} \tag{2}$$

where σ is the triboelectric charge density (0.00281 μC cm^{-2} (Figure S4, Supporting Information)), ε_0 is the vacuum permittivity (8.85 × 10^{-12} F m^{-1}), ζ is the damping factor of the TENG system (0.34 by experimental measurement (Figure S5, Supporting Information)), and a is the acceleration of the electrodynamic shaker (a typical value of g/50 (where g is the gravitational acceleration)). The theoretical result of the V_{oc} at the resonance frequency is calculated to be 464.2 V, which is larger than the experimental result of 287.4 V. The difference probably results from the assumptions made in the analytical model and non-ideal factors in the experiment. First, Equation (2) is based on an assumption that the two contact surfaces are smooth. However, surface modification by nanomaterials is used in the real case, leading to a substantially enhanced contact area and thus to a higher triboelectric charge density. The value of triboelectric charge density submitted into Equation (2) is obtained experimentally. Therefore, it is very likely to result in an overestimation of the theoretical V_{oc}. In addition, non-ideal factors, such as humidity and particle contaminations in the air, which are not considered in the theoretical model, may potentially have a negative impact on the actual voltage output.

As shown in Figure 3d, the output current at the resonance frequency has an alternating behavior with asymmetrical amplitudes. It is found that the larger peaks correspond to the process in which the two contact surfaces move apart after collision, while the smaller ones are generated as the two surfaces approach each other. Given the same amount of charges transported back and forth, the faster separation is expected to produce larger current peaks than the slower approach, leading to the asymmetry. It is worth noting that the peak value of the current is different for discharge and charge cycles, but the integration over time, namely the amount of induced charges, is almost the same (Figure S4, Supporting Information), indicating no leakage current. At the resonance frequency, the total amount of induced charges reaches the maximum value of 6.2 μC within 2 s. The output charge only slightly reduces at other vibration frequencies below 120 Hz (Figure S6, Supporting Information), further indicating that the TENG has a considerably wide working bandwidth as a vibration energy harvester.

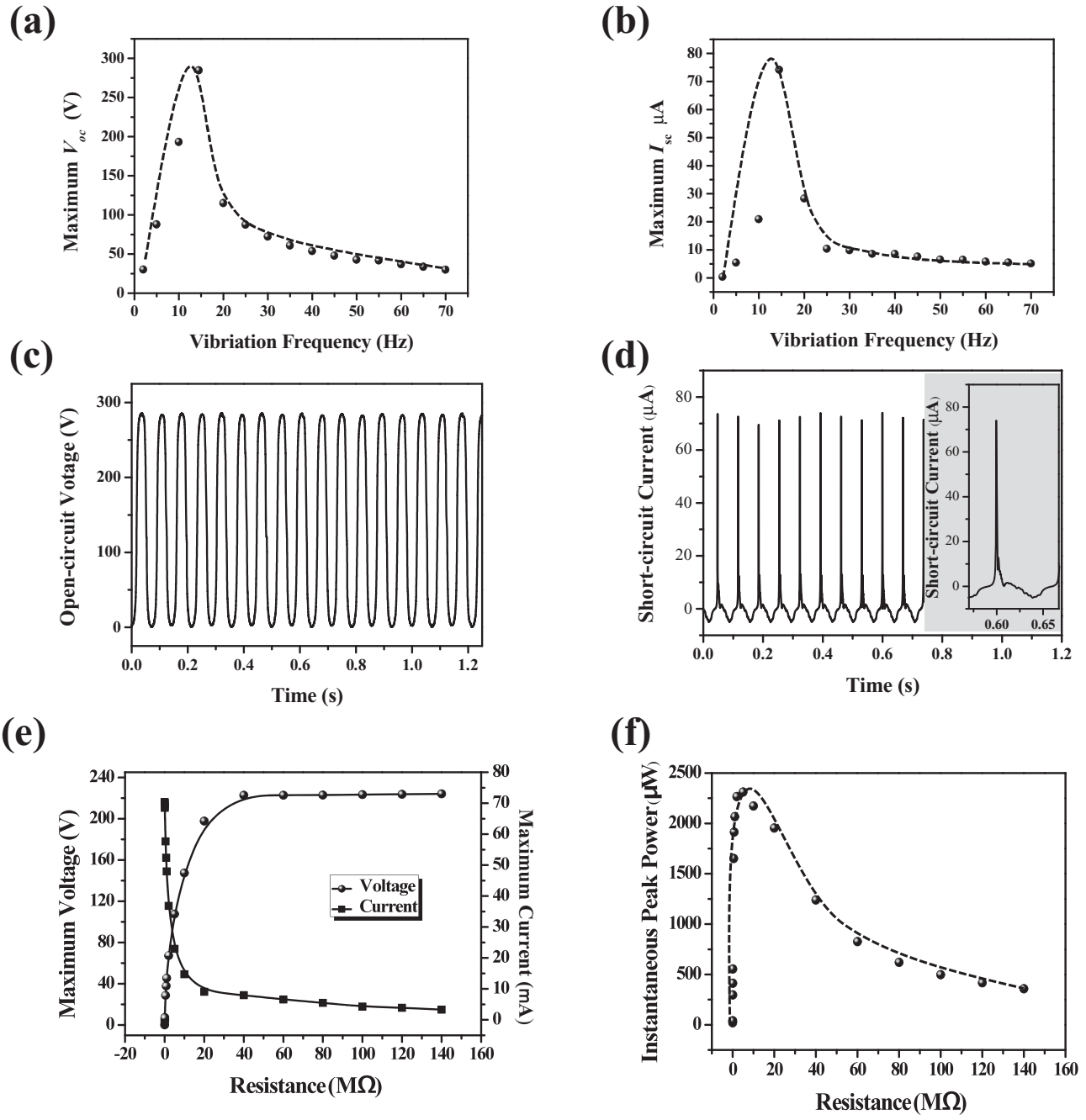

Figure 3. Electrical measurement results of a harmonic-resonator-based TENG. a) Open-circuit voltage (V_{oc}) as a function of vibration frequency. The curve is a fitted result. b) Short-circuit current (I_{sc}) as a function of vibration frequency. The curve is a fitted result. c) Open-circuit voltage (V_{oc}) at vibration frequency of 14.5 Hz. d) Short-circuit current (I_{sc}) at vibration frequency of 14.5 Hz. Inset: enlarged view of one cycle. e) Dependence of the voltage and current output on the external load resistance. The points represent peak value of electric signals while the lines are the fitted results. f) Dependence of the peak power output on the resistance of the external load, indicating maximum power output when R = 5 MΩ. The curve is a fitted result.

Resistors were utilized as external loads to further investigate the output power of the TENG at the resonance frequency. As displayed in Figure 3e, the current amplitude drops with increasing load resistance owing to the ohmic loss, while the voltage follows a reverse trend. As a result, the instantaneous peak power (V^2_{peak}/R) is maximized at a load resistance of 5 MΩ, corresponding to a peak power density of 726.1 mW m^{-2} (Figure 3f).

The harmonic-resonator-based TENG demonstrated here has four unique characteristics. First, a major challenge for previous TENGs was the relatively low current compared to high voltage output.[13–22] Compared with all other TENGs that relied

Adv. Mater. 2013,
DOI: 10.1002/adma.201302397

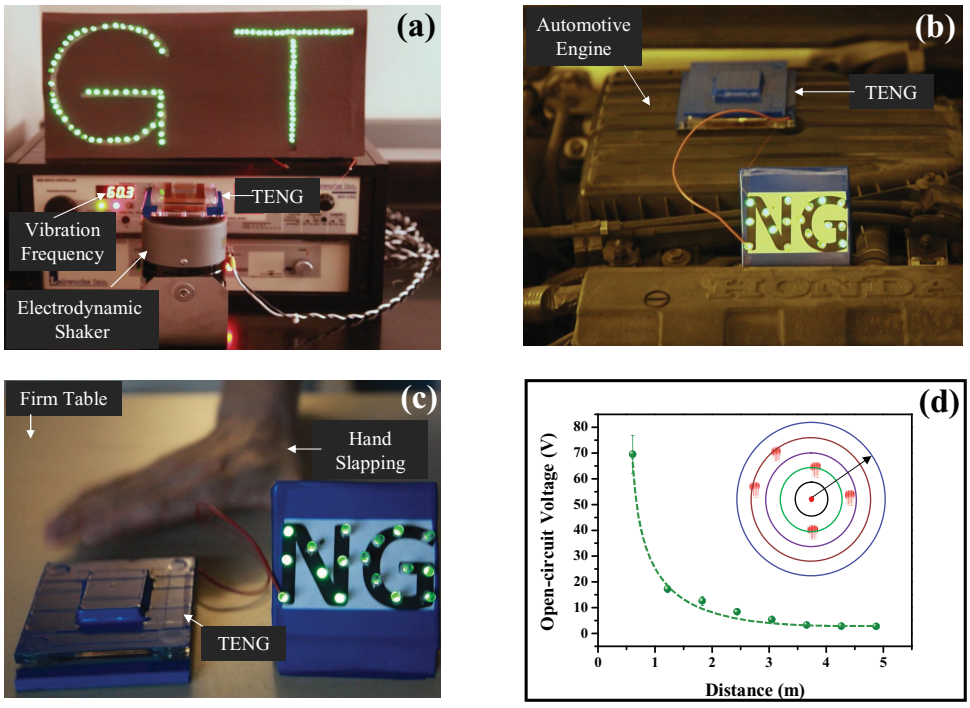

Figure 4. Demonstration of the harmonic-resonator-based TENG as a sustainable power source and self-powered active vibration sensor. a) Photograph that shows TENG is working on an electrodynamic shaker at the vibration frequency of 60 Hz, which is the United States national power frequency. About 100 LEDs light up simultaneously without stroboflash perceived by a naked eye. b) Photograph that shows TENG works on an automotive engine. When the car starts up, the "NG" lights up simultaneously. c) Photograph that shows TENG works when a human hand slaps a firm table. Owing to the table vibration, about 20 LEDs light up simultaneously. d) TENG acts as an active vibration sensor for distance measurement as well as ambient vibration detection. When a human walks towards the TENG, which is fixed on the floor, the output signal is exponentially increased.

on contact mode,[13–19] this harmonic-resonator-based TENG is the first of its kind that allows output current in high frequency, leading to greatly enhanced effective current (overall charge per unit time). Second, to promote the triboelectrification and to increase the effective contact area between the two contact surfaces, aluminum nanopores and PTFE nanowires are created as surface modifications. The rational design, coupled with nanomaterials modification, greatly increases the effective contact area and thus the triboelectric charges. As a comparison, the electrical measurement of a harmonic-resonator-based TENG without PTFE nanowires and aluminum nanopores surface modification is demonstrated in Figure S7, Supporting Information, which shows that the short-circuit current output with nanomaterials modification is increased to about 2.1 times of that for the TENG without nano-materials surface modification. Third, at the original position, the upper substrate rests at a critical state where the elastic force from the springs is completely compensated by the gravitational force from the upper substrate, making the TENG extremely sensitive to even tiny external vibrational excitation. Fourth, unique operating principle of the harmonic-resonator-based TENG allows easy packaging of the device, which could not be achieved by previous TENGs. Since the TENG does not rely on direct interaction with external force, it can be readily sealed in an outer container as long as one substrate is anchored onto the container. Thus, it can be applied outdoor and even in circumstances with harsh environment and extreme conditions, thereby greatly expanding its applicability.

To prove the capability of the harmonic-resonator-based TENG as a sustainable power source and an active vibration sensor, four sets of practical applications were demonstrated (see the videos in Supporting Information). First, as shown in **Figure 4**a, the TENG was excited by an electrodynamic shaker at a vibration frequency of 60 Hz, lighting up almost 100 light-emitting diode (LED) bulbs simultaneously and continuously without observable stroboflash. Second, as shown in Figure 4b, the TENG was mounted onto an automotive engine. It successfully harvests vibrational energy from the operating engine and powers about 20 LED bulbs simultaneously. The third practical application shows that the TENG, sitting on a table, generates electricity and drives small electronics as impact from a nearby human palm initiates vibration of the table (Figure 4c). Last, as demonstrated in Figure 4d, the TENG can also act as an active vibration sensor for detecting ambient vibration. When a human naturally walks beside the TENG that is placed on the floor, electric output can successfully be obtained. With the maximum effective range of 5 m, the electric output amplitude is exponentially related to the distance between the TENG and the footstep. These demonstrated applications prove that the TENG is sensitive to small ambient vibrations, making it suitable to a wide range of circumstances for either energy-harvesting or sensing purposes: for example, highways, bridges, and tunnels.

In summary, we present a harmonic-resonator-based TENG as a sustainable power source and an active vibration sensor. Rationally designed structure of the TENG, coupled with

nanomaterials modification, allows superior performance in ambient vibration energy harvesting. It produces a uniform quasi-sinusoidal signal output with an open-circuit voltage up to 287.4 V, a short-circuit current amplitude of 76.8 μA, and a peak power density of 726.1 mW m^{-2}. It can effectively respond to input vibration frequency from 2 to 200 Hz with a considerably wide working bandwidth of 13.4 Hz. The harmonic-resonator-based TENG is very sensitive to small ambient vibrations, such as an operating automobile engine, it can also act as an active vibration sensor for ambient vibration detection. This work not only presents a new principle in the field of vibration energy harvesting but also greatly expands the applicability of TENGs as power sources for self-sustained electronics.

Experimental Section

Nanopore-Based Aluminum Surface Modification: Relying on 3% mass fraction oxalic acid ($H_2C_2O_4$) electrolyte, the electrochemical anodization was applied on the aluminum thin film. It was anodized under a bias voltage of 30 V for 5 hours with a platinum plate acting as the cathode. After that, the alumina layer was etched away in a solution of chromic acid (20 g l^{-1}) at 60 °C for 2 h.

Nanowire-Based PTFE Surface Modification: A layer of 100 nm copper was first deposited onto the 50 μm thick PTFE film for the etching process. Subsequently, the ICP reactive ion etching was applied to fabricate the aligned PTFE nanowires on the surface. O_2, Ar, and CF_4 gases were injected into the ICP chamber with a flow ratio of 10.0, 15.0, and 30.0 sccm, respectively. A large density of plasma was generated by a power source of 400 W. And another power source of 100 W was used to accelerate the plasma ions. The copper-coated PTFE film was etched for 40 s to get the PTFE nanowires with an average length of ≈1.5 μm.

Fabrication of the Harmonic-Resonator-Based TENG: To fabricate the TENG, two pieces of acrylic were shaped by a laser cutter as substrates with dimensions of 3.2 inches × 3.2 inches × 0.25 inches. Four holes were drilled at each corner for spring installation. A layer of 100 nm aluminum was deposited on the one substrate in a size of 2 inches × 3 inches as the top electrode. 100 nm copper-coated PTFE in a size of 2 inches × 3 inches was assembled on the other acrylic substrate with PTFE facing the aluminum on the top substrate. Subsequently, four springs was anchored to connect the top and bottom substrate with the springs' elastic force exactly compensating the gravitational force of the top plate and the two plates just contact with each other. Finally, lead wires were utilized to connect the top and bottom electrode for electrical measurement.

Supporting Information

Supporting Information is available from the Wiley Online Library or from the author.

Acknowledgements

J.C. and G.Z. contributed equally to this work. The research was supported by US Department of Energy, Office of Basic Energy Sciences, Division of Materials Sciences and Engineering under Award DE-FG02-07ER46394, the US National Science Foundation and the Knowledge Innovation Program of the Chinese Academy of Sciences (KJCX2-YW-M13).

Received: May 26, 2013
Revised: July 17, 2013
Published online:

[1] Z. L. Wang, J. H. Song, *Science* **2006**, *312*, 242.
[2] X. D. Wang, J. H. Song, J. Liu, Z. L. Wang, *Science* **2007**, *316*, 102.
[3] Y. Qin, X. D. Wang, Z. L. Wang, *Nature* **2008**, *451*, 809.
[4] R. S. Yang, Y. Qin, L. M. Dai, Z. L. Wang, *Nat. Nanotechnol.* **2009**, *4*, 34.
[5] S. Xu, Y. Qin, C. Xu, Y. G. Wei, R. S. Yang, Z. L. Wang, *Nat. Nanotechnol.* **2010**, *5*, 366.
[6] X. L. Bai, Y. M. Wen, J. Yang, P. Li, J. Qiu, Y. Zhu, *J. Appl. Phys.* **2012**, *111*, 07A938.
[7] P. D. Mitcheson, P. Miao, B. H. Stark, E. M. Yeatman, A. S. Holmes, T. C. Green, *Sens. Actuators, A* **2004**, *115*, 523.
[8] L. Wang, F. G. Yuan, *Smart Mater. Struct.* **2008**, *17*, 045009.
[9] S. P. Beeby, M. J. Tudor, N. M. White, *Meas. Sci. Technol.* **2006**, *17*, 175.
[10] D. Shen, J. H. Park, J. H. Noh, S. Y. Choe, S. H. Kim, D. J. Kim, *Sens. Actuators A* **2009**, *154*, 103.
[11] Y. K. Tan, in *Sustainable Energy Harvesting Technologies – Past, Present and Future*, InTech, Rijeka, Croatia **2011**, Ch.7.
[12] H. Kulah, K. Najafi, *IEEE Sens. J.* **2008**, *8*, 261.
[13] F. R. Fan, Z. Q. Tian, Z. L. Wang, *Nano Energy* **2012**, *1*, 328.
[14] F. R. Fan, L. Lin, G. Zhu, W. Z. Wu, R. Zhang, Z. L. Wang, *Nano Lett.* **2012**, *12*, 3109.
[15] G. Zhu, C. F. Pan, W. X. Guo, C. Y. Chen, Y. S. Zhou, R. M. Yu, Z. L. Wang, *Nano Lett.* **2012**, *12*, 4960.
[16] S. H. Wang, L. Lin, Z. L. Wang, *Nano Lett.* **2012**, *12*, 6339.
[17] G. Zhu, Z. H. Lin, Q. S. Jing, P. Bai, C. F. Pan, Y. Yang, Y. S. Zhou, Z. L. Wang, *Nano Lett.* **2013**, *13*, 847.
[18] P. Bai, G. Zhu, Z. H. Lin, Q. S. Jing, J. Shen, G. Zhang, J. S. Ma, Z. L. Wang, *ACS Nano* **2013**, *7*, 3713.
[19] X. S. Zhang, M. D. Han, R. X. Wang, F. Y. Zhu, Z. H. Li, W. Wang, H. X. Zhang, *Nano Lett.* **2013**, *13*, 1168.
[20] G. Zhu, J. Chen, Y. Liu, P. Bai, Y. S. Zhou, Q. S. Jing, C. F. Pan, Z. L. Wang, *Nano Lett.* **2013**, *13*, 2282.
[21] S. H. Wang, L. Lin, Y. N. Xie, Q. S. Jing, S. M. Niu, Z. L. Wang, *Nano Lett.* **2013**, *13*, 2226.
[22] L. Lin, S. H. Wang, Y. N. Xie, Q. S. Jing, S. M. Niu, Y. F. Hu, Z. L. Wang, *Nano Lett.* **2013**, *13*, 2916.
[23] J. Lowell, A. C. Rose-Innes, *Adv. Phys.* **1980**, *29*, 947.
[24] R. G. Horn, D. T. Smith, *Science* **1992**, *256*, 362.
[25] R. G. Horn, D. T. Smith, A. Grabbe, *Nature* **1993**, *366*, 442.
[26] L. H. Tang, Y. W. Yang, *Appl. Phys. Lett.* **2012**, *101*, 094102.
[27] X. Y. Wang, S. Palagummi, L. Liu, F. G. Yuan, *Smart Mater. Struct.* **2013**, *22*, 055016.
[28] K. Ashraf, M. H. M. Khir, J. O. Dennis, Z. Baharudin, *Smart Mater. Struct.* **2013**, *22*, 049601.
[29] G. S. P. Castle, *J. Electrost.* **1997**, *40*, 13.
[30] E. Nemeth, V. Albrecht, G. Schulert, F. Simon, *J. Electrostat.* **2003**, *58*, 3.
[31] R. V. Dukkipati, *Vibration Analysis*, Alpha Science International, Harrow, UK **2004**, Ch. 2.